Quantum Strings in Quantum Spin Ice

Yuan Wan and Oleg Tchernyshyov

Quantum strings in quantum spin ice

Yuan Wan and Oleg Tchernyshyov

Department of Physics and Astronomy, Johns Hopkins University, Baltimore, MD 21218

We study quantum spin ice in an external magnetic field applied along a $\langle 100 \rangle$ direction. When quantum spin fluctuations are weak, elementary excitations are quantum strings with monopoles at their ends manifested as multiple spin-wave branches in the dynamical structure factor. Strong quantum fluctuations make the string tension negative and give rise to the deconfinement of monopoles. We discuss our results in the light of recent neutron scattering experiments in $Yb_2Ti_2O_7$.

The quest for novel quantum phases and elementary excitations is one of the central themes in condensed-matter physics. The notion of an elementary excitation is conventionally associated with a point-like object, as the term *quasiparticle* implies. A natural question is whether elementary excitations in quantum materials could resemble *strings*, rather than particles. String excitations were recently found in spin ice $Dy_2Ti_2O_7$ [1, 2], a frustrated ferromagnet with fractionalized excitations known as magnetic monopoles [3, 4]. In an applied magnetic field, excitations are strings of misaligned spins connecting two monopoles of opposite charge.

Conventional spin ice is a classical magnet with Ising spins [5]. Therefore, magnetic monopoles and strings in it are classical objects whose dynamics are due to thermal fluctuations. In this letter, we propose that string excitations with inherent quantum dynamics may exist in quantum spin ice, a new family of spin-ice materials exemplified by $Tb_2Ti_2O_7$ and $Yb_2Ti_2O_7$ [6][7]. In these compounds, spins exhibit substantial quantum fluctuations. We demonstrate that, in a certain regime of coupling constants, elementary excitations of quantum spin ice are strings with quantum dynamics. The calculated dynamical structure factor $S(\omega, \mathbf{k})$ reveals multiple branches of excitations that correspond, loosely speaking, to strings of different lengths. As the applied field increases, these branches gradually separate and the lowest one evolves into a magnon. We connect these findings to recent experiments on neutron scattering in $Yb_2Ti_2O_7$ [8, 9].

We begin with a toy model of quantum spin ice on the two-dimensional checkerboard lattice, Fig. 1. The point of departure is classical spin ice, in which spins have projections $S_i^z = \pm 1/2$ on local directions $\hat{\mathbf{z}}_i$ shown in Fig. 1a. Magnetic charge on a crossed plaquette (planar tetrahedron) is defined as $Q_{\boxtimes} = -\epsilon_{\boxtimes} \sum_{i \in \boxtimes} S_i^z$, with $\epsilon_{\boxtimes} = \pm 1$ for sublattice A (B). The ground states of the classical spin-ice Hamiltonian,

$$H_0 = \sum_{\boxtimes} \sum_{\langle ij \rangle \in \boxtimes} J S_i^z S_j^z = \sum_{\boxtimes} J Q_{\boxtimes}^2 / 2 + \text{const}, \quad (1)$$

obey the Bernal-Fowler rule, $Q_{\boxtimes} = 0$, on every tetrahedron [5]. Next we apply a weak magnetic field in the ac
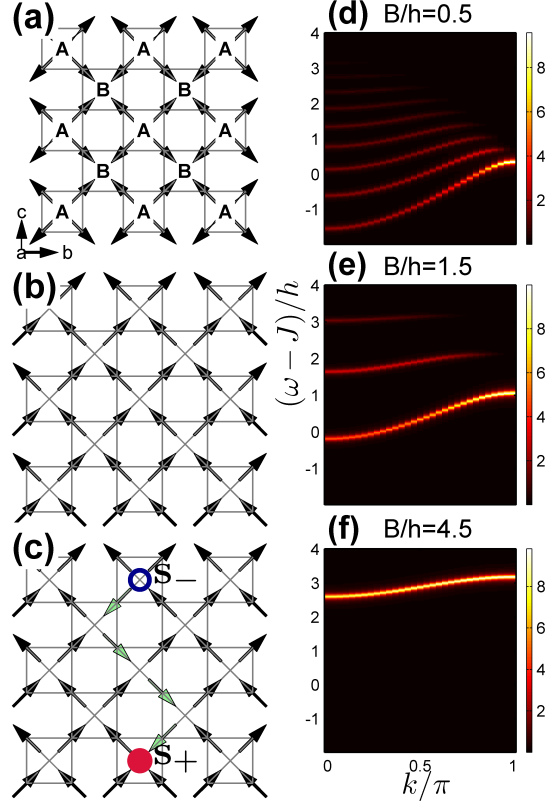

FIG. 1: (a) The checkerboard lattice. A and B denote two symmetrically inequivalent planar tetrahedra, and arrows the local $\hat{\mathbf{z}}_i$ directions. (b) The fully-polarized state when the field is applied in the c direction. Arrows denote the spin orientations. (c) A string of flipped spins (light green) binding a $Q = +1$ monopole (red solid circle) and a $Q = -1$ one (open blue circle). (d, e, f) $-\text{Im} S^{aa}(\omega, \mathbf{k})$ for $k_b = 0$. $B/h = 0.5$, 1.5, and 4.5 respectively.

plane. In the local frames, the perturbation reads

$$H_1 = -\sum_i (h S_i^x + B \eta_i S_i^z). \quad (2)$$

Here we chose the local y-axes to be orthogonal to the field and introduced cosines $\eta_i \equiv \hat{\mathbf{c}} \cdot \hat{\mathbf{z}}_i = (-1)^{c_i}/\sqrt{2}$. The Zeeman term (2) has two effects. Its longitudinal component B breaks the degeneracy of ice states and favors
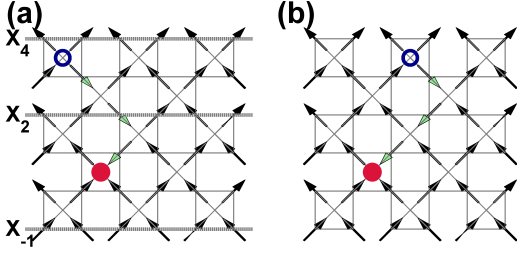
FIG. 2: Definition of X_c operators. The operator X_2 changes the orientation of the string segment with $c = 2$ from $\mathbf{l}$ to $\mathbf{r}$ in state (a) and results in a new state (b). The operators $X_{-1,5}$ fall outside the range of the string and act trivially on (a).

a fully magnetized state, Fig. 1b. The transverse component h induces quantum fluctuations of spins. We treat B and h as independent parameters in the toy model.

Flipping a single spin in the fully magnetized state creates two monopoles with $Q = \pm 1$, which can be pulled further apart. The process creates a string of spins aligned against the field and connecting the monopoles, Fig. 1c. For $h = 0$, the energy of a string with n segments is $J + Bn/\sqrt{2}$. For weak fields, the Hilbert space thus sep-

arates into near-degenerate subspaces with a fixed number of strings. The transverse part of the Zeeman term (2) mixes states in the same subspace through quantum tunneling, inducing quantum motion of strings. We use degenerate perturbation theory in the subspace with a single string to construct an effective theory of its quantum dynamics.

The shape of a string is specified by its segments $\{\mathbf{s}_1, \mathbf{s}_2 \ldots \mathbf{s}_n\}$, or $\{\mathbf{s}_i\}$ for short, which take on the values $\mathbf{r} \equiv (0, 1, 1)$ and $\mathbf{l} \equiv (0, -1, 1)$ in the abc-frame. The string thus propagates upwards in Fig. 1c from the $Q = +1$ monopole at $\mathbf{s}_+$ to the $Q = -1$ monopole at $\mathbf{s}_-$. Because of the constraint $\mathbf{s}_- - \mathbf{s}_+ = \sum_{i=1}^{n} \mathbf{s}_i$, the state of a string is fully specified by its shape and location of one of the ends, $|\mathbf{s}_+, \{\mathbf{s}\}\rangle$. We introduce a hybrid basis with fixed shape $\{\mathbf{s}_i\}$, c-coordinate of the monopole c_+, and the b-component of the total momentum k_b:

$$|k_b, c_+, \{\mathbf{s}_i\}\rangle = \sum_{b_+} e^{ik_b(b_+ + b_-)/2}|b_+, c_+, \{\mathbf{s}_i\}\rangle. \quad (3)$$

To the first order in h, the motion of a string involves removing or adding a segment at one of the ends, with an effective Hamiltonian

$$
\begin{aligned}
H_{\text{eff}}|c_+, \{\mathbf{s}_1 \ldots \mathbf{s}_n\}\rangle &= (J + nB/\sqrt{2})|c_+, \{\mathbf{s}_1 \ldots \mathbf{s}_n\}\rangle - (h/2)e^{ik_b b_n/2}|c_+, \{\mathbf{s}_1 \ldots \mathbf{s}_{n-1}\}\rangle - (h/2)e^{-ik_b b_1/2}|c_+ + 1, \{\mathbf{s}_2 \ldots \mathbf{s}_n\}\rangle \\
&\quad - (h/2)\sum_{\mathbf{s}_{n+1}} e^{-ik_b b_{n+1}/2}|c_+, \{\mathbf{s}_1 \ldots \mathbf{s}_{n+1}\}\rangle - (h/2)\sum_{\mathbf{s}_0} e^{ik_b b_0/2}|c_+ - 1, \{\mathbf{s}_0 \ldots \mathbf{s}_n\}\rangle. \quad (4)
\end{aligned}
$$

Here b_i stands for the b-component of the vector $\mathbf{s}_i$. We have omitted the momentum index to simplify the notation.

When $k_b = 0$, diagonalization of H_{eff} is simplified by the presence of multiple reflection symmetries. Define the parity operator X_c that switches between the $\mathbf{l}$ and $\mathbf{r}$ orientations of the segment with coordinate c and keeps all other segment variables $\mathbf{s}_i$ intact (Fig.2), e.g.

$$X_c|c_+, \ldots \mathbf{s}_{c-c_+}, \mathbf{l} \ldots\rangle = |c_+, \ldots \mathbf{s}_{c-c_+}, \mathbf{r} \ldots\rangle. \quad (5)$$

When X_c falls outside the range of the string, $c_+ < c < c_-$, it acts on the vacuum state, which is symmetric, so we set $X_c|c_+, \{\mathbf{s}\}\rangle = +|c_+, \{\mathbf{s}\}\rangle$ in this case. It can be seen that $X_c^2 = 1$ and $[X_c, X_{c'}] = 0$. Although X_c does not preserve the coordinate of the other end of the string $\mathbf{s}_-$, at $k_b = 0$ its horizontal displacement makes no difference; therefore, $[X_c, H_{\text{eff}}] = 0$. Thus, all $k_b = 0$ eigenstates of H_{eff} can be classified by their parities under $\{X_c\}$ and H_{eff} becomes block-diagonal. The most important states have all even parities, $X_c = +1$. An all-even state of a

string of length n and longitudinal momentum k_c is

$$|k_c, n\rangle = 2^{-n/2} \sum_{c_+} \sum_{\mathbf{s_1} \ldots \mathbf{s_n}} e^{ik_c(c_+ + c_-)/2}|c_+, \{\mathbf{s}_1 \ldots \mathbf{s}_n\}\rangle. \quad (6)$$

For them, the Hamiltonian (4) simplifies,

$$H_{\text{eff}}|n\rangle = \left(J + \frac{nB}{\sqrt{2}}\right)|n\rangle - \sqrt{2}h\cos\frac{k_c}{2}\sum_{m=n\pm1}|m\rangle. \quad (7)$$

The above is equivalent to the one-dimensional problem of a particle on a lattice subject to a constant force $-B/\sqrt{2}$ and a hard wall at $n = 0$. For $B \ll h$, we use the continuum approximation to find the spectrum:

$$E_j(k_c) = J - 2\sqrt{2}\left|h\cos\frac{k_c}{2}\right| + \lambda_j\left|\frac{\sqrt{2}}{2}B^2 h\cos\frac{k_c}{2}\right|^{1/3}. \quad (8)$$

Here λ_j are roots of the Airy function. When $B \gg h$, the lowest eigenstate is a single misaligned spin with the dispersion

$$E_1(k_c) = J + \frac{B}{\sqrt{2}} - \frac{\sqrt{2}h^2}{B}(1 + \cos k_c). \quad (9)$$

Likewise, H_{eff} can be diagonalized in odd-parity sectors [10].

Strings can be directly observed in neutron scattering experiments. A scattered neutron flips a spin in the fully-polarized background, creating a string of length 1. The intensity of scattering is proportional to the overlap between a length-1 string and a string eigenstate of H_{eff} squared. Fig. 1 shows the dynamical structure factor $-\text{Im}S^{aa}(\omega, \mathbf{k})$ at several values of B/h for $k_b = 0$. For this direction of $\mathbf{k}$, the spectral weight comes solely from states with all-even parities, $X_m = +1$. For $B \lesssim h$, the spectrum consists of overlapping bands, whereas for $B \gg h$ the bands separate and the spectrum becomes dominated by the shortest string consisting of a single flipped spin, in essence a magnon.

For general $\mathbf{k}$, we used the Lanczos method to calculate the spectrum numerically and found similar behavior. Parities X_c are no longer good quantum numbers; therefore, more bands appear in the spectrum.

The case of three-dimensional quantum spin ice, with $S = 1/2$ spins on the pyrochlore lattice, proceeds along similar lines. The most general exchange Hamiltonian is written in local axes (Fig. 3a) as [11]

$$H_{\text{pyro}} = \sum_{\langle ij \rangle} J_{zz} S_i^z S_j^z - J_{z\pm}[S_i^z(\zeta_{ij}S_j^+ + \zeta_{ij}^* S_j^-) + (i \leftrightarrow j)]$$
$$- J_\pm(S_i^+ S_j^- + h.c.) - J_{\pm\pm}(\zeta_{ij}^* S_i^+ S_j^+ + h.c.) \quad (10)$$

Here $\zeta_{ij} = \zeta_{ji}$ are phase factors, and i and j labeling spin sublattices 0 to 3. Specifically, $\zeta_{01} = \zeta_{23} = -1$, $\zeta_{02} = \zeta_{13} = \exp(i\pi/3)$, $\zeta_{03} = \zeta_{12} = \exp(-i\pi/3)$, and $\zeta_{ii} = 0$. The J_{zz} term describes classical spin ice, whereas the three remaining terms create quantum fluctuations.

A magnetic field applied in the [001] direction adds the Zeeman term $-B \sum_i \alpha_i S_i^x + \beta_i S_i^y + \gamma_i S_i^z$, with the cosines

$$\alpha_{0,3} = -\alpha_{1,2} = \frac{g_{xy}}{g_z\sqrt{6}}, \qquad \beta_{0,3} = -\beta_{1,2} = \frac{g_{xy}}{g_z\sqrt{2}},$$
$$\gamma_{0,3} = -\gamma_{1,2} = \frac{1}{\sqrt{3}}, \qquad (11)$$

where g_{xy} and g_z are the principal components of the g-tensor. In what follows we assume that the spin-ice term J_{zz} dominates and treat the rest of the terms as perturbations. The z Zeeman term favors the fully-magnetized state (Fig. 3b). Excitations are open strings connecting a pair of monopoles with $Q = \pm1$. Magnetic charge is defined as usual, $Q_\boxtimes \equiv -\epsilon_\boxtimes \sum_{i \in \boxtimes} S_i^c$, where $\boxtimes$ stands for a tetrahedron and $\epsilon_\boxtimes = \pm1$ for tetrahedra of sublattice A (B).

The state of a string $|\mathbf{s}_+, \{\mathbf{s}\}\rangle$ is again parametrized by the location of its $Q = +1$ end $\mathbf{s}_+$ and by its shape $\{\mathbf{s}\} \equiv \{\mathbf{s}_1, \mathbf{s}_2 \ldots \mathbf{s}_n\}$. String segments $\mathbf{s}_i$ have four possible orientations: $\mathbf{b}_0 = (1,1,1)/4$, $\mathbf{b}_1 = (-1,1,1)/4$, $\mathbf{b}_2 = (1,-1,1)/4$, and $\mathbf{b}_3 = (-1,-1,1)/4$. A segment with orientation $\mathbf{b}_0$ or $\mathbf{b}_3$ must be followed by a segment with orientation $\mathbf{b}_1$ or $\mathbf{b}_2$, and vice versa.
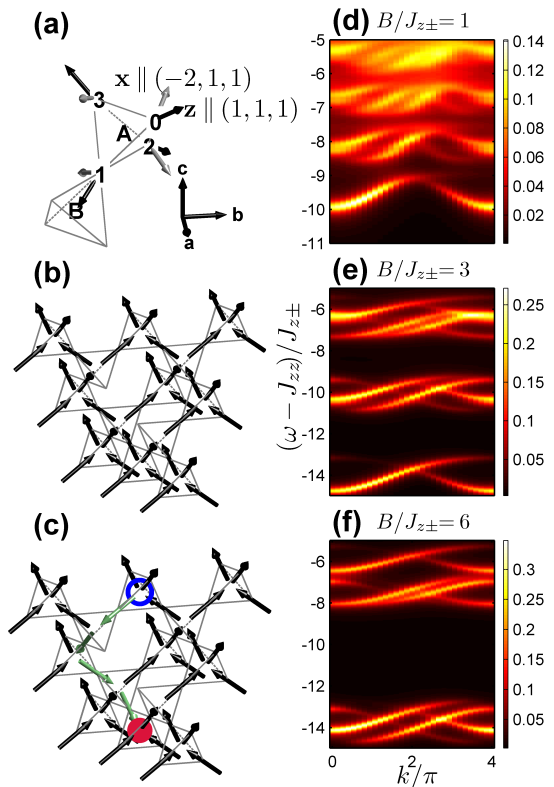

FIG. 3: (a) A and B denote two inequivalent tetrahedra in the pyrochlore lattice and $0 \sim 3$ four sublattices. The gray and black arrows show the local $\hat{\mathbf{x}}$ and $\hat{\mathbf{z}}$ directions. The abc vectors specify the local frame for one sublattice. (b) The fully-polarized state when the field is applied in the c direction. Arrows show the spin orientations. (c) A string of flipped spins (light green) binding a $Q = +1$ monopole (red solid circle) and a $Q = -1$ one (blue open circle) (d,e,f) The neutron scattering spectra for the momentum transfer $\mathbf{k} \parallel \mathbf{B}$. $B/J_{z\pm} = 1,3$, and 6 respectively.

The effective Hamiltonian in the subspace of a single string is

$$H_{\text{eff}} = -\sqrt{3}J_{z\pm}K_1 - J_\pm K_2 - 2J_{\pm\pm}K_3 + V \quad (12)$$

Kinetic terms K_1 and K_2 describe first and second-neghbor hopping of the string ends, whereas K_3 describes the hopping of a string of length 1. $V = J + nB/\sqrt{3}$ for a string of length n. The explicit form of K_i is given in [10].

Fig. 3 shows the neutron scattering spectrum $-(\text{Im}S^{aa} + \text{Im}S^{bb})$ calculated with the aid of Lanczos diagonalization, for momentum transfer $\mathbf{k} \parallel \mathbf{B}$ [10]. We set $J_\pm = J_{\pm\pm} = 0.36J_{z\pm}$, and $g_{xy}/g_z = 2.4$ as in Yb$_2$Ti$_2$O$_7$ [8]. The spectral features resemble those of 2D strings (Fig. 1). The branches gradually separate as the string tension increases with B. When $J_{z\pm} \sim J_\pm \sim J_{\pm\pm} \ll B \ll J_{zz}$, the monopole dynamics is dominated by the x and y Zeeman terms whereas the string tension is provided by the z term.
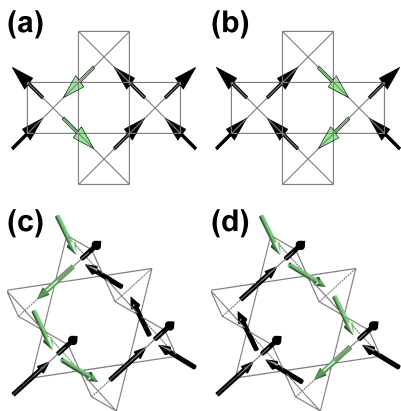
FIG. 4: Loop-flipping processes in (a,b) checkerboard lattice $|\mathbf{lr}\rangle \leftrightarrow |\mathbf{rl}\rangle$ and (c,d) pyrochlore lattice $|\mathbf{b_2 b_3 b_1}\rangle \leftrightarrow |\mathbf{b_1 b_3 b_2}\rangle$.

To the first order in perturbations $J_{z\pm,\pm,\pm\pm}$, transverse fluctuations induce the motion of a string's ends. At higher-orders in these couplings, the string's shape can change as well. The process involves the simutaneous reversal of spins around a closed loop (minimal length 4 in square ice and 6 in pyrochlore ice) [12, 13]. In square ice, a state $|\ldots\mathbf{lr}\ldots\rangle$ turns into $|\ldots\mathbf{rl}\ldots\rangle$ and vice versa, Fig. 4. When the position of the monopole and the anti-monopole are both fixed, these fluctuations can be mapped onto a $S = 1/2$ XY chain [14], with spin values $\tau^z = \pm 1/2$ representing $\mathbf{r}$ and $\mathbf{l}$ segments, and the Hamiltonian

$$H_{\text{fluc}} = V_{\text{2D}} \sum_{i=1}^{n-1} (\tau_i^+ \tau_{i+1}^- + \text{H.c.}), \qquad (13)$$

where $V_{\text{2D}} = \mathcal{O}(h^4/J^3)$. Quantum fluctuations reduce tension of the string to $B/\sqrt{2} - 2|V_{\text{2D}}|/\pi$. When the applied field is below the critical strength $B_c = 2\sqrt{2}|V_{\text{2D}}|/\pi$, the energy cost for string excitations is negative and the fully-polarized state becomes unstable. A similar transition occurs in the pyrochlore quantum spin ice, where a string can be mapped onto an XY chain with second-neighbor interactions only [Fig. 4(c) and (d)],

$$H_{\text{fluc}} = V_{\text{3D}} \sum_{i=1}^{n-1} (\tau_{2i-1}^+ \tau_{2i+1}^- + \tau_{2i}^+ \tau_{2i+2}^- + \text{H.c.}). \quad (14)$$

The string tension is reduced by $2|V_{3D}|/\pi$. When B is below the critical value $B_c = 2\sqrt{3}|V_{\text{3D}}|/\pi$, the polarized state becomes unstable.

The fate of the ground state below B_c depends on the dimensionality. On the one hand, the zero field ground state of the pyrochlore spin ice in the perturbative regime $J_{z\pm,\pm,\pm\pm} \ll J_{zz}$ is a $U(1)$ spin liquid with deconfined monopoles[13]. Therefore, the transition at B_c could be associated with deconfinement of monopoles. On the other hand, given that the compact quantum electrodynamics is always confined in $2D$ [15], the $B = 0$ ground

state of the 2D quantum spin ice is likely another confined phase separated from the fully-polarized state by the transition at B_c.

In the quantum spin-ice material $\mathrm{Yb_2Ti_2O_7}$, the couplings associated with quantum spin fluctuations, viz. $J_{z\pm}$, $J_\pm$, and $J_{\pm\pm}$, are comparable with the spin-ice term J_{zz} [8]. Therefore, perturbative calculations don't apply to it directly. Nonetheless, the physical picture is expected to hold beyond the perturbative regime if the material lies in the phase that is adiabatically connected to the magnetized state. A recent experiment indicates the ground state of $\mathrm{Yb_2Ti_2O_7}$ is a ferromagnet [9]. The spontaneous magnetization in a $\langle 100 \rangle$ direction acts as a "molecular field," creating nonzero string tension even in the absence of an external field. We expect that strings in quantum spin ice can be detected by neutrons and photons. It would be particularly interesting to observe a continuous evolution of string excitations in an increasing magnetic field applied along a $\langle 100 \rangle$ direction.

[1] L. D. C. Jaubert, J. T. Chalker, P. C. W. Holdsworth, and R. Moessner, Phys. Rev. Lett. **100**, 067207 (2008).
[2] D. J. P. Morris, D. A. Tennant, S. A. Grigera, B. Klemke, C. Castelnovo, R. Moessner, C. Czternasty, M. Meissner, K. C. Rule, J.-U. Hoffmann, K. Kiefer, S. Gerischer, D. Slobinsky, and R. S. Perry, Science **326**, 411 (2009).
[3] I. A. Ryzhkin, J. Exp. Theor. Phys. **101**, 481 (2005).
[4] C. Castelnovo, R. Moessner, and S. L. Sondhi, Nature **451**, 42 (2007).
[5] M. Gingras, in *Introduction to Frustrated Magnetism* (Springer, 2011).
[6] H. R. Molavian, M. J. P. Gingras, and B. Canals, Phys. Rev. Lett. **98**, 157204 (2007).
[7] J. D. Thompson, P. A. McClarty, H. M. Rønnow, L. P. Regnault, A. Sorge, and M. J. P. Gingras, Phys. Rev. Lett. **106**, 187202 (2011).
[8] K. A. Ross, L. Savary, B. D. Gaulin, and L. Balents, Phys. Rev. X **1**, 021002 (2011).
[9] L.-J. Chang, S. Onoda, Y. Su, Y.-J. Kao, K.-D. Tsuei, Y. Yasuia, K. Kakurai, and M. R. Lees, arXiv:1111.5406 .
[10] EPAPS Document No.xxxx.
[11] S. H. Curnoe, Phys. Rev. B **75**, 212404 (2007).
[12] G. T. Barkema and M. E. J. Newman, Phys. Rev. E **57**, 1155 (1998).
[13] M. Hermele, M. P. A. Fisher, and L. Balents, Phys. Rev. B **69**, 064404 (2004).
[14] J. B. Kogut, D. K. Sinclair, R. B. Pearson, J. L. Richardson, and J. Shigemitsu, Phys. Rev. D **23**, 2945 (1981).
[15] A. Polyakov, Nucl. Phys. B **120**, 429 (1977).